Journal of Hazardous Materials 377 (2019) 52–61

Contents lists available at ScienceDirect

Journal of Hazardous Materials

journal homepage: www.elsevier.com/locate/jhazmat

Auto-ignition behaviors of nitromethane in diluted oxygen in a rapid compression machine: Critical conditions for ignition, ignition delay times measurements, and kinetic modeling interpretation

Meng Yang, Yingtao Wu, Chenglong Tang*, Yang Liu, Zuohua Huang

State Key Laboratory of Multiphase Flow in Power Engineering, Xi'an Jiaotong University, Xi'an, 710049, China

ARTICLE INFO

Keywords:
Nitromethane
Rapid compression machine
Critical conditions for ignition
Ignition delay times
Kinetic

ABSTRACT

In this work, the weakest thermodynamic conditions for the auto-ignition of mixtures containing nitromethane were experimentally determined by using the rapid compression machine facility. Results show there is a narrow weak ignition region between ignition and non-ignition. The weak ignition region would disappear with the increase of the EOC (end of compression) pressure and nitromethane concentration. In addition, the ignition delay times for successful auto-ignition for different nitromethane concentrations and equivalence ratio mixtures were measured and compared. Results show that the dependence of nitromethane ignition on the equivalence ratio is weak. Subsequently, the measured ignition delay time data were employed to validate several kinetic models in literature and our previous model shows better agreement with experimental results, as well as other available literature data. Sensitivity analysis for the model reveals the importance of unimolecular decomposition and H-abstraction reactions for the ignition delay times in the temperature range studied herein. Finally, critical conditions for nitromethane ignition under extended conditions that are beyond the ability of the experimental facility were predicted.

1. Introduction

Safety testing of energetic materials such as explosives or propellants is highly desirable. To measure thermal properties as time to explosion (ignition delay time) and weakest thermodynamic condition for thermal explosion is very important for the construction of the cook-off models and for the safety issue during the storage, transportation and handling of energetic material [1].

As an energetic material, nitromethane (NM or CH_3NO_2) is the simplest nitro-paraffin and has been selected as prototype compound to study the combustion behaviors of practical explosives and propellants such as research department explosive (RDX) [2] and hydroxyazanium nitrate (HAN)-based monopropellant [3]. NM has been used as a monopropellant and a liquid explosive. In addition, it can be used as an additive for internal combustion engines, which can increase the power output and reduce soot emission [4–6]. Furthermore, as an explosive compound, accidental leakage of nitromethane into air forms explosive and flammable mixtures [7,8], which leads to serious risk of safety, which are mainly caused by thermal or shock stimulations.

Extensive theoretical and experimental investigations have been conducted to evaluate the explosive hazards based on nitromethane at different levels [9–16]. The processes of detonation in pure NM have been studied by plate impact experiments under a steady one-dimensional strain for pressures from 8.5 to 12 GPa [13]. The results not only reveal the main steps of the classical homogeneous model, but also show that the build-up process is extremely complex. In addition, the explosion process of mist/air and mist/dust/air of NM has been reported by Liu et al. [17]. For the pure gaseous nitromethane mixtures, cellular structure of detonation [8,18] and the influence of nitromethane concentration on ignition energy [7] in gaseous nitromethane mixtures have been reported. However, the lowest temperature for auto-ignition of a given mixture containing nitromethane has not been reported.

In addition, understanding the auto-ignition behaviors of nitromethane is important for the hazardous evaluation of this energetic material. The auto-ignition characteristics are primarily controlled by the dissociation or oxidation kinetics of nitromethane under different thermodynamics conditions. As such, a number of theoretical and experimental researches [19–27] on the decomposition and oxidation kinetics of nitromethane have been conducted. These work showed that the main nitromethane decomposition paths include the direct C–N bond cleavage to generate CH_3 and NO_2, and O—N bond cleavage to

* Corresponding author.
E-mail address: chenglongtang@mail.xjtu.edu.cn (C. Tang).

https://doi.org/10.1016/j.jhazmat.2019.05.036
Received 1 February 2019; Received in revised form 28 April 2019; Accepted 15 May 2019
Available online 23 May 2019

generate CH_3O and NO. Furthermore, ignition delay times of CH_3NO_2/O_2 /Ar and CH_3NO_2/O_2 /N_2 mixture have also been measured by Mathieu et al. [25] and Nauclér et al. [26], for temperatures higher than around 900 K. These two papers both found a two-stage ignition behavior. Meanwhile, Mathieu et al. developed a detailed kinetic mechanism, which showed reasonable performance in predicting their measured ignition delay times at high temperature. Recently, we have also measured the ignition delay times of CH_3NO_2/O_2/Ar mixtures at high temperatures (1200–2000 K). Additionally, we developed a detailed kinetic mechanism for nitromethane oxidation through ab-initio calculations, which shows good agreement with our measured ignition delay times as well as the literature data, including laminar burning velocities and ignition delay times at high temperature [27]. However, there has been no report of the experimental and simulated combustion parameters of nitromethane in low to intermediate temperature range.

Since the critical condition that leads to nitromethane auto-ignition provides some guidelines for the safety evaluation of nitromethane, and understanding of the auto-ignition onset is of merit for designing new safety testing methodology for energetic materials. Our first objective of this work is to experimentally determine the critical thermodynamic conditions (lowest temperature) for the auto-ignition of a given mixture containing nitromethane. Secondly, for the successful auto-ignition cases, ignition under a given thermodynamic condition is initiated after a certain period of ignition delay time, which represents the overall reactivity of the mixture, thus we will provide ignition delay data of nitromethane, in the low to intermediate temperature range for different pressures and mixture conditions by using a rapid compression machine facility. The data will then be used to validate our recently proposed kinetic model that includes updated low temperature chemistry, after which sensitivity and reaction pathway analysis based on our validated model will be presented to interpret the ignition kinetics. Finally, by using the validated model, the critical thermodynamic conditions at extended conditions that are beyond the ability of the experimental facility will be predicted.

2. Experimental specifications

2.1. Setup and procedures

Ignition delay times of nitromethane (Aladdin, 99.0%) were measured using the rapid compression machine facility. Fig. 1 shows the schematic image of the rapid compression machine system. Details of the RCM system have been introduced in our previous work [28]. Briefly, the system consists of six parts, including the high pressure air tank, the driving chamber, the hydraulic chamber, the compression chamber, the combustion chamber and the control and data acquisition system. The pressure evolution inside the combustion chamber section is recorded by a recess-mounted piezoelectric pressure transducer (Kistler 6125C) combined with a charge amplifier (Kistler 5018A). Details of the operation of the rapid compression machine can be found in the Supplementary material.

The reactive and non-reactive mixtures are prepared in two heated separate stainless vessels according to the partial pressure of each component. A relative manometer (OMEGA DPG4000) with an accuracy of 10 Pa is used to measure the partial pressure of each component. It is noted that the partial pressure of the liquid nitromethane is assured to be less than 1/3 of its saturated pressure at the vessel temperature so as to avoid condensation effect. We note that the saturated vapor pressure of nitromethane at room temperature (293 K) is small (3.71 kPa). The mixture preparation system including the mixture vessel, the pipelines and the reaction chamber is heated with temperature fixed at 328 K. At this temperature, the vapor pressure is 20 kPa [29]. The maximum partial pressure of nitromethane in the experiment is assured to be less than 7 kPa. 8 mixtures are prepared and the components of each tested mixture are summarized in Table 1. In these mixtures, Mix 1–4 and Mix 8 at 15 bar are used to study the critical conditions for nitromethane ignition; While Mix 5–8 is used to study the chemical kinetic of nitromethane. Because the nitromethane concentration is low in this experiment, the explosion pressure after ignition is expected to be low and thus the experiment is safe. In addition, to find the appropriate diluents composition for reliable ignition delay time determination in rapid compression machine (typically 10˜200 ms), several tests have been performed. When using Ar as the diluents, ignition happens very fast and for some cases ignition happens even before EOC. When N_2 is used as diluents, ignition is not observed within 200 ms. The reason is that nitrogen has large specific heat, which leads to low temperature after compression. As such, the Ar/N_2 ratio is then fixed at 3:1. Furthermore, the highest temperature in the present study is limited by the shortest ignition delay times that can be validly extracted from the pressure trace. The corresponding non-reactive mixture experiments were conducted by replace O_2 using the same mole fraction of N_2 to obtain volume-time histories.

2.2. Definition of ignition delay times

Fig. 2 shows a typical pressure evolution history for the ignition of $CH_3NO_2/O_2/N_2$/Ar mixture (solid line) and the corresponding non-reactive mixture (dash line). The ignition delay in this work is defined as

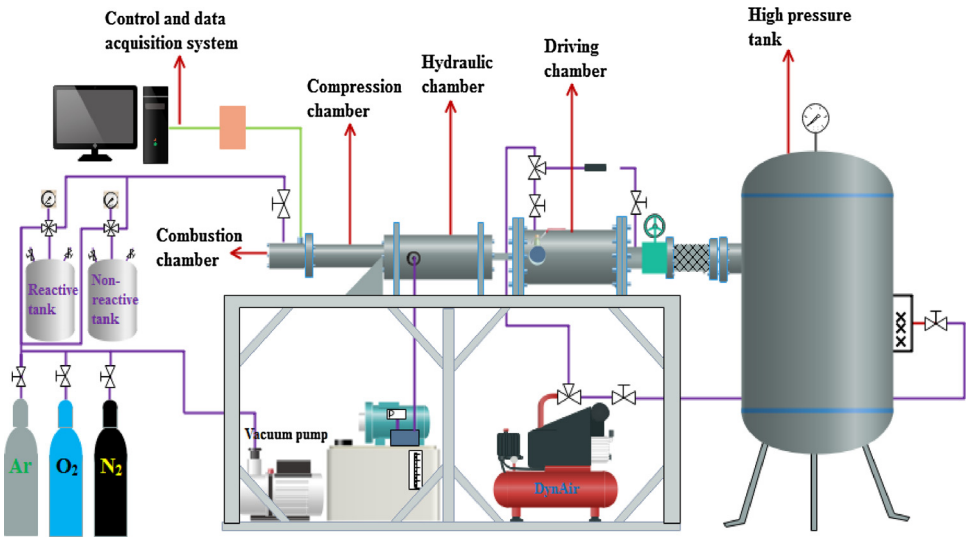

Fig. 1. Schematic of the rapid compression machine system for the present ignition delay time measurements.

Table 1
Test conditions and reactant mixtures.

Mix #	φ	P_c	Ar/N_2	Mole fraction (%)		
				[NM]	[O_2]	[N_2]
1	2.0	10-30	3	1.00	0.625	24.59
2	2.0	15	3	0.5	0.3125	24.80
3	2.0	15	3	1.5	0.9375	24.39
4	2.0	15	3	2.5	1.5625	23.98
5	1.0	15, 30	3	1.00	1.25	24.44
6	0.5	15, 30	3	2.00	5.00	23.25
7	1.0	15, 30	3	2.00	2.50	23.875
8	2.0	15, 30	3	2.00	1.25	24.19

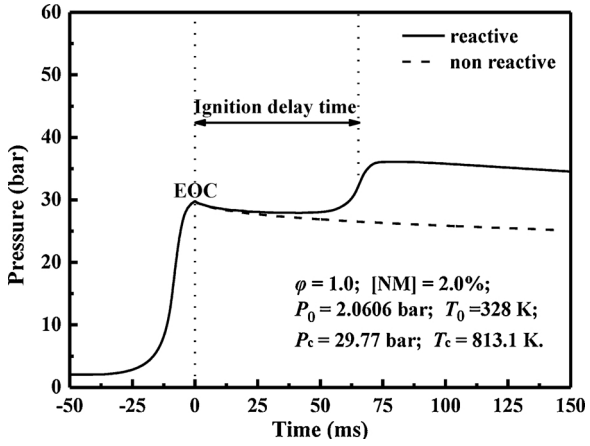

Fig. 2. Typical pressure trace and definition of ignition delay time.

the time from the EOC to the onset of ignition, which is recognized as the instant with the maximum pressure rise rate. The P_c and T_c at EOC are used as the reference conditions for reporting ignition delay times [30,31]. T_c is determined by P_c through the isentropic relation.

$$\int_{T_0}^{T_c} \frac{\gamma}{\gamma - 1}\frac{dT}{T} = \ln\left(\frac{P_c}{P_0}\right) \quad (1)$$

where P_c is the measured EOC pressure, T_c is the temperature at that time, T_0 and P_0 are the temperature and pressure before compression, and γ is the temperature dependent specific heat ratio.

The uncertainty of ignition delay measurement is estimated to be less than 12%, using the method reported in Refs. [32,33]. The uncertainty in ignition delay time is primarily resulted from the pressure measurement (including initial pressure by the pressure gauge, the dynamic pressure by the pressure transducer and charge amplifier) and the uncertainties in temperature measurement (dynamic pressure and the initial temperature). Uncertainty in the mixture composition is generally very small and is neglected. In this work, to avoid accidental errors, each experiment is repeated at least two times. By using the independent parameters methodology [34], the uncertainty in T_c is estimated to be less than 5 K. All the experimental data and the detailed uncertainty analysis can be seen in the Supplementary material.

Numerical simulations for ignition delay times were conducted using the zero-dimensional closed homogeneous reactor model in CHEMKIN-PRO. The volume-time profiles are adopted to account for the heat loss, while applying the zero-dimensional adiabatic core assumption. The ignition delay time in simulation is defined as the time interval between the start of calculation and the maximum pressure rise rate on the simulated pressure history.

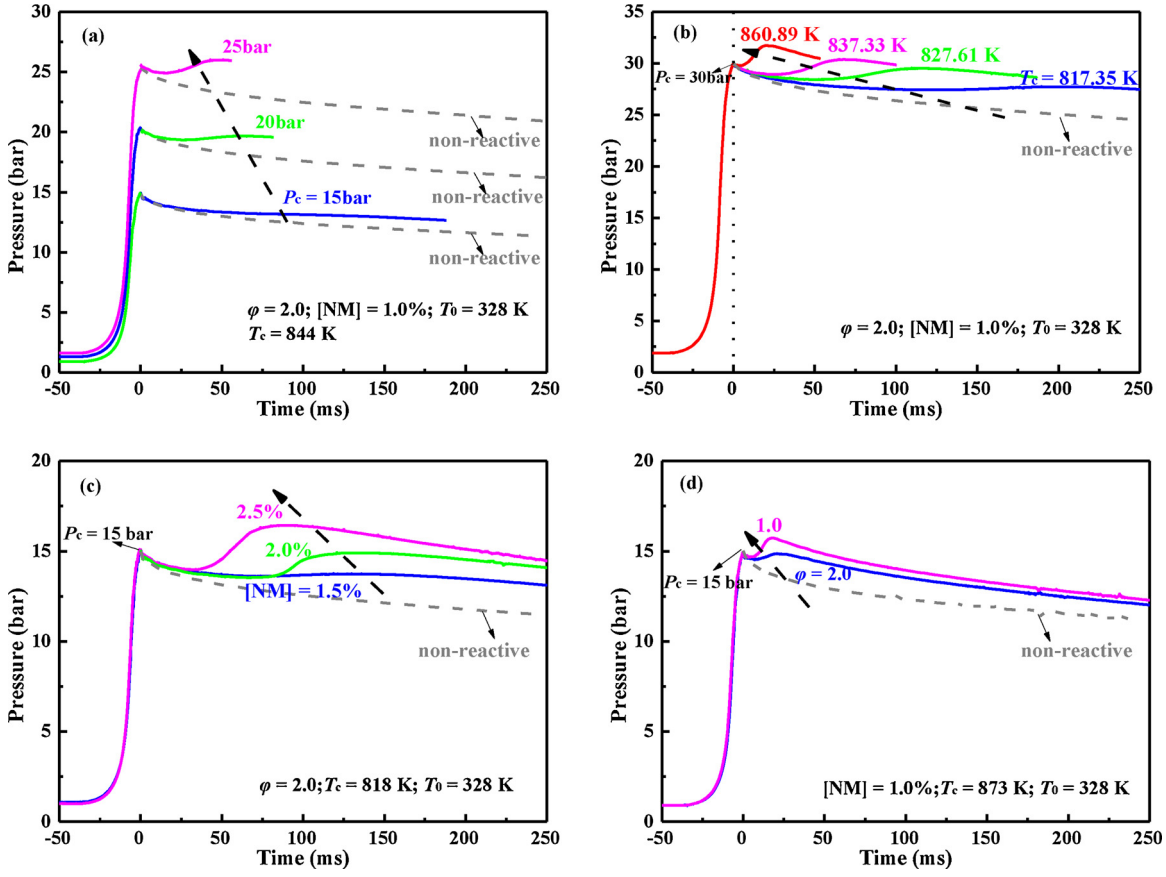

Fig. 3. Raw pressure histories at: (a) different EOC pressures; (b) different EOC temperatures; (c) different NM concentrations; (d) different equivalence ratios.

3. Results and discussion

3.1. Critical thermodynamic conditions for ignition

Fig. 3 shows the typical raw pressure histories of reactive (solid line) and non-reactive (dash line) tests at different EOC conditions. It can be seen that when nitromethane concentration is low, there will be an interesting slow pressure rise ratio phenomenon after EOC, which differs from common ignition. Fig. 3 (a) presents pressure-time histories with different EOC pressures. The pressure rise rate will increase and ignition delay time will decrease with the EOC pressure increase. Compared with the non-reactive pressure profile at EOC pressure of 15 bar, there is a weak ignition. That may be attributed to the low specific energy of nitromethane (about 11.3 MJ/kg) [35]. Fig. 3 (b) presents the evolution of pressure with different EOC temperatures. With the EOC temperature increasing, the ignition delay time will decrease. In addition, the nitromethane mixture goes through the process which is from non-ignition to weak ignition to ignition eventually with the temperature increase. The variation of pressure histories with the NM concentration is shown in Fig. 3(c). When the nitromethane concentration increases from 1.5% to 2.5%, the ignition explosion pressure and pressure rise ratio increase significantly and the ignition delay time decreases. Fig. 3(d) presents the evolution of pressure at different equivalence ratios. The ignition delay time decreases slightly with the equivalence ratio decreasing from 2.0 to 1.0. It illuminates that the reactivity of nitromethane is not sensitive to the amount of oxygen.

According to the raw pressure traces of nitromethane at low concentrations, three distinct regions were identified: 1. Ignition region. In this region, the ignition was defined as an obvious pressure rise after compression; 2. Weak ignition region. In this area, the rise of pressure is not distinct after the compression end point. However, the trace of pressure is higher than non-reactive history. That is to say there is a slow chemical reaction in this region; 3. Non-ignition region. Therefore, an ignition region diagram is presented for NM concentration of 1%, equivalence ratio of 2.0 and different EOC pressure, as shown in Fig. 4. It can be seen that the critical temperature of ignition increases with the EOC pressure decreasing, such as that at P_c = 15 bar (about 850 K) is higher than that at P_c = 30 bar (about 820 K). Increasing pressure is conducive to the occurrence of ignition. In this condition, the weak ignition region exists at some specific temperatures and pressures. As the pressure in EOC is increased to 30 bar, the weak ignition region becomes narrow. Because when pressure increases, the collision frequency of mixture gas molecules increases. Then chemical reaction will be accelerated. The weak ignition region will disappear as the pressure continues to increase. While, when the pressure is very low, high

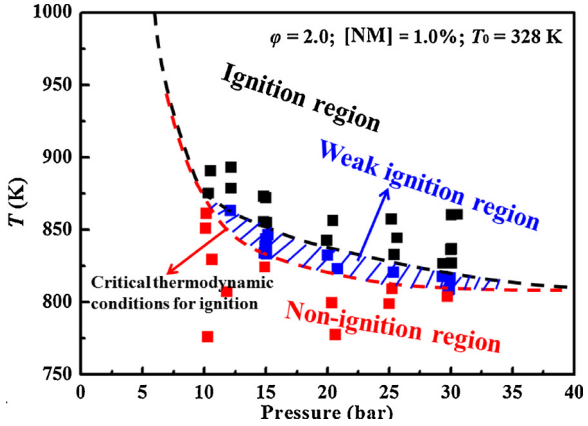

Fig. 4. Test points and regions about ignition at different temperatures (in EOC), P_c = 10–30 bar. (black symbols: ignition; blue symbols: weak ignition; red symbols: non-ignition). (For interpretation of the references to colour in this figure legend, the reader is referred to the web version of this article.)

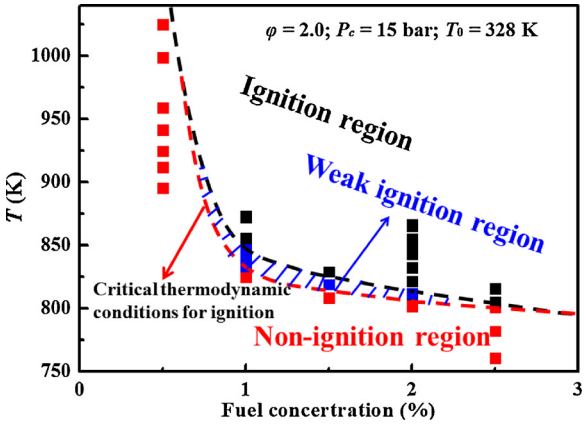

Fig. 5. Test points and regions about ignition at different temperatures (in EOC), P_c = 15 bar, [NM] = 0.5%–2.5%. (black symbols: ignition; blue symbols: weak ignition; red symbols: non-ignition). (For interpretation of the references to colour in this figure legend, the reader is referred to the web version of this article.)

temperature will make the nitromethane mixture ignition, and there is no weak ignition region. This is because the high temperature will increase the internal energy of the mixture, which favors the reactivity such that the weak ignition region will also vanishes at high temperature.

Fig. 5 shows test points and predicted regions about ignition at different temperatures, different nitromethane concentrations and pressure of 15 bar. First, the critical ignition temperature of nitromethane mixture decreases with the concentration growing from 0.5% to 2.5%. Due to low specific energy, the ignition of nitromethane will have weak heat release at low NM concentrations due to slow chemical reaction. Weak ignition region will appear at low NM concentrations. As the NM concentration further grows, the weak ignition region becomes narrow. When the heat release can maintain combustion, the weak ignition region will disappear. In addition, when the NM concentration is less than 1%, it can be predicted that there will only be ignition region and non-ignition region. Since concentration is very low, there are no slow chemical reactions. Only when high temperature at EOC provide enough energy for mixture, it will ignition at the same time. Also there will be a critical NM concentration at which the ignition can't happen even at very high temperature. And for the NM concentration of 0.5%, there is no ignition at the temperature range from 895 to 1025 K.

3.2. Ignition delay times: measurements and correlations

For the test experimental conditions in the ignition region, ignition delay time can be obtained, as in Fig. 2. Figs. 6–8 present all the measured ignition delay times as a function of inverse temperature for different equivalence ratios, NM concentrations and pressures. Across all test conditions in this work, it can be seen that the negative temperature coefficient behavior, which is typically observed for hydrocarbon fuels such as n-heptane and iso-octane in the low to intermediate temperature range, is absent for nitromethane. The measured IDTs in logarithm increase quasi-linearly with the inverse temperature, indicating its Arrhenius temperature dependence. These ignition delay times (τ_{ign}, in ms) data are then correlated as a function of the experimental conditions, including the pressure (p, in bar), NM mole fraction ([NM]), equivalence ratio (φ) and temperature (T, in K) through,

$$\tau_{ign} = Ap^{B}[NM]^{C}\varphi^{D}\exp(E_a/RT) \quad (2)$$

where $R = 1.986 \times 10^{-3}$ kcal/(mole·K) is the universal gas constant, and E_a is the global activation energy in kcal/mol. The fitting result is shown in Eq. (3), with R^2 values above 0.97. The correlation of Eq. (3)

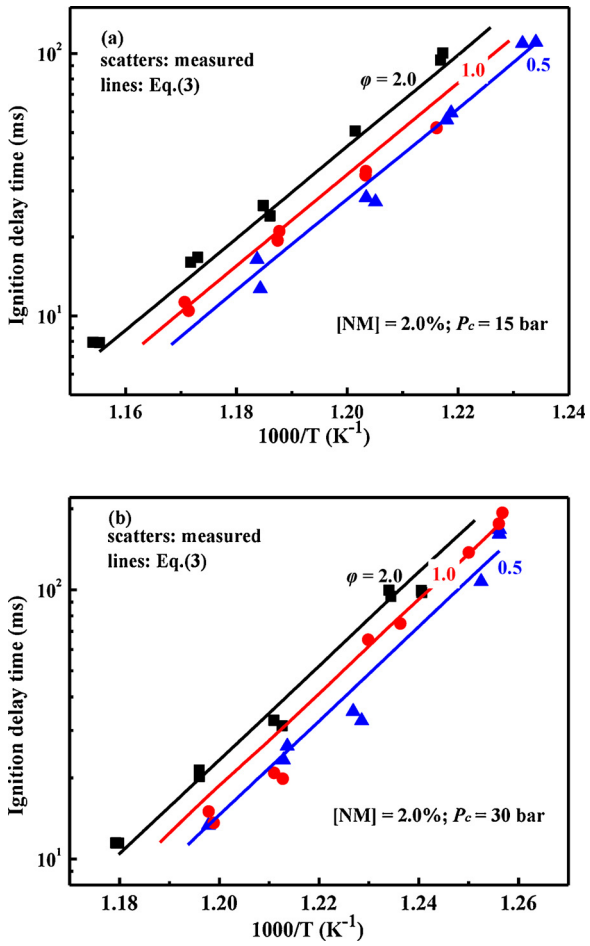

Fig. 6. Ignition delay times for [NM] = 2.0%, φ = 0.5-2.0. (a) P_c = 15 bar, (b) P_c = 30 bar.

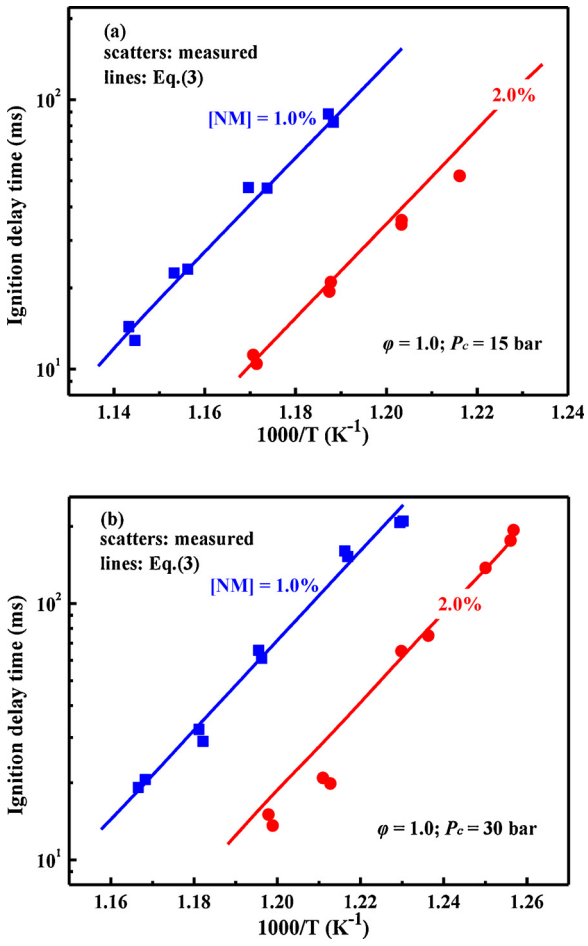

Fig. 7. Ignition delay times for φ = 1.0, [NM] = 1.0% and 2.0%. (a) P_c = 15 bar, (b) P_c = 30 bar.

was also presented in Fig. 6–8. Though the ignition delay times at φ = 1.0 and NM concentration of 2.0% are slightly over-predicted, the correlation can give general good agreement against experimental results both quantitatively and qualitatively.

$$\tau_{ign} = 10^{-21.665} p^{-0.916} [NM]^{-1.963} \varphi^{0.334} \exp(79.821/RT) \quad (3)$$

3.2.1. The effect of equivalence ratio

For the NM concentration of 2.0%, the effect of equivalence ratio on the ignition delay times of nitromethane at 15 bar and 30 bar is respectively illustrated in Fig. 6(a) and (b). It can be seen that the ignition delay times increase with increasing equivalence ratio at these two pressures. When the equivalence ratio increases with fixed NM concentration, the oxygen fraction decreases and the inert has a higher concentration, resulting in a higher ignition delay times. Previously for ignition delay times study in different shock tubes, similar effect of the equivalence ratio was observed [25,27].

3.2.2. The effect of NM concentration and pressure

The influence of NM concentration and the pressure on the ignition delay times of nitromethane was also presented in Figs. 7 and 8. The effect of NM concentration and pressure are very straightforward because the increase of the NM concentration and pressure increases the reactant NM concentration. For fixed pressure shown in Fig. 7, the ignition delay times decrease sharply with the NM concentration increasing. With the increase of the NM concentration, the oxygen concentration also increases for fixed equivalence ratio, faster reaction rate (assume global reaction k_{gl} $[NM]^m[O_2]^n$, where k_{gl} is the temperature dependent rate constant, m and n is reaction order) is then expected due to increased.

Fig. 8 (a) shows experimental ignition delay times and fitted lines with Eq. (3) at equivalence ratio of 0.5 and pressure of 15 and 30 bar. It can be seen that the increase in pressure induces increased reactivity. Fig. 8 (b)-(c) presents the same trend under equivalence of 1.0 and 2.0. This is because higher pressure leads to higher reaction rate due to increased reactant concentration.

3.3. Comparisons of different kinetic mechanisms

3.3.1. Low temperature ignition delay times in this work

The experimental results were compared with calculations using the kinetic mechanisms developed by Brequigny et al. [36], Mathieu et al. [25] and our previously developed model containing low temperature chemistry [27]. The Brequigny model, involving 88 species and 701 reactions, has been validated against laminar flame speeds, species profiles at low pressure and high temperature shock tube ignition delay times. The Mathieu model, involving 166 species and 1204 reactions, has been validated against high temperature ignition delay times, pyrolysis species profiles and laminar flame speeds. Our mechanism, involving 171 species and 1219 reactions, has been validated against high temperature ignition delay and laminar flame speeds. In addition, low temperature reactions have been updated including such as $CH_3NO_2 + CH_3 = CH_2NO_2 + CH_4$, $CH_3NO_2 + OH = CH_2NO_2 + H_2O$ and $CH_3NO_2 + H = CH_2NO_2 + H_2$. It is noted that all three mechanisms included the oxidation sub-model of nitromethane. But the models of Gao et al. as well as the models from Mathieu et al. and Brequigny

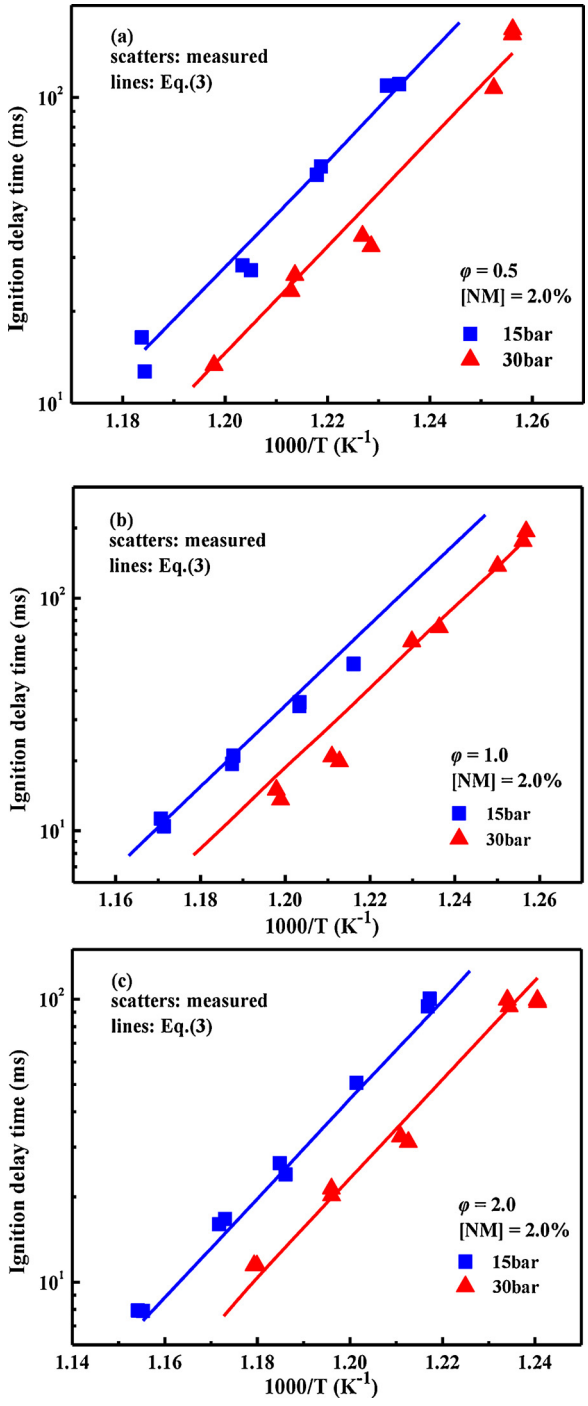

Fig. 8. Ignition delay times for [NM] = 2.0% and P_c = 15 bar and 30 bar. (a) φ = 0.5, (b) φ = 1.0 and (c) φ = 2.0.

et al. have not been sufficiently validated against low to intermediate temperature ignition delay of nitromethane.

Fig. 9 (a) presents the measured and calculated stoichiometric mixture ignition delay times of nitromethane with NM concentration of 1% at 15 bar and 30 bar. Generally, all three models can predict the trend of ignition delay times with temperature variation. The Brequigny model gives an over-prediction (less than 50% for all two pressures). At 15 bar, the predictions of Mathieu model have a good agreement with measured ignition delay times. At pressure of 30 bar, however, Mathieu model substantially underestimates the ignition delay times. The Gao model gives generally better predictions for ignition delay times at the two pressures, though at relatively lower temperature, predictions of

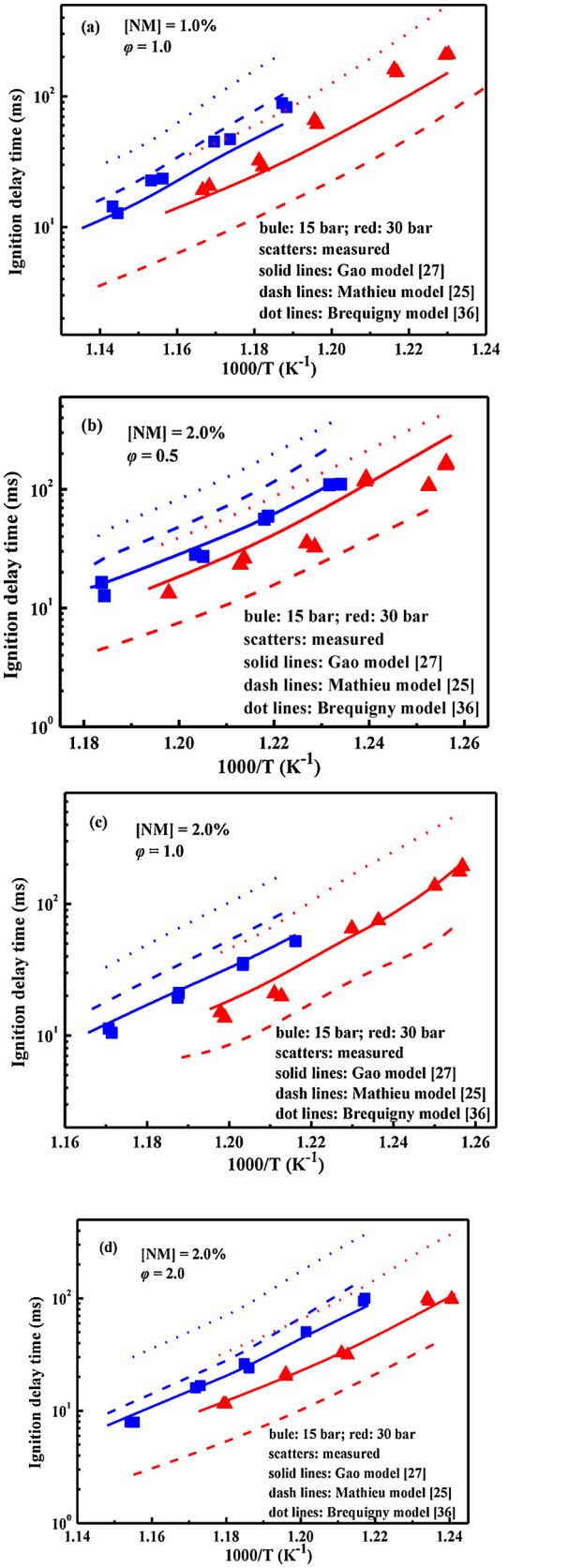

Fig. 9. Experimental and computed ignition delay times of nitromethane: (a) φ = 1.0, [NM] = 1.0%; (b) φ = 0.5, [NM] = 2.0%; (c) φ = 1.0, [NM] = 2.0%; (d) φ = 2.0, [NM] = 2.0%.

the ignition delay times are slightly lower than measurements. We note that in Section 3.1, there is a narrow weak ignition region at NM concentration of 1% at relatively lower temperature. The pressure rise is slow, which affects the recognition of ignition onset and results in a larger ignition delay time. So when NM concentration is less than 1%, the measurements of ignition delay time are not used for comparison with the mechanism predictions.

Fig. 9(b)–(d) compares the measured and predicted ignition delay times of nitromethane at higher NM concentration (2%), different pressures and equivalence ratios. For this NM concentration mixture, there is almost no weak ignition region, as shown in Fig. 5. Therefore, the measured ignition delay times can be more accurately determined. In Fig. 9(b)–(d), similar to the trend observed in Fig. 9(a), the predictions using Brequigny model and Mathieu model show noticeable disagreement with the experimental data. Gao model again shows good performance in predicting the experimental ignition delay times.

3.3.2. CO and NO mole fraction evolution in literature

To further compare and validate the three mechanisms of nitromethane, the time evolution of NO and CO concentrations during the pyrolysis of the diluted nitromethane in a shock-tube is simulated and compared with the data collected by Hsu and Lin [21]. For the 0.25% CH_3NO_2/Ar mixture as shown in Fig. 10 (a), the Brequigny model [36] and Mathieu model [25] under-predict (more than 50%) noticeably the NO and CO evolution during pyrolysis. In comparison, the Gao model [27] predicts both NO and CO profiles with better agreements.

When nitromethane concentration is 0.4%, there is a reasonable prediction from three mechanisms as shown in Fig.10 (b). In detail, the CO profile is well captured by the Gao model, whereas the Mathieu model slightly under-predicts the CO formation. The equilibrium NO is over-estimated by all the models by 15%.

For 0.76% CH_3NO_2, the NO profile is relatively well predicted, and CO profile is under-predicted (around 30%) by the Brequigny model and Mathieu model, while the Gao model over-predicts NO profile by up to 20% but predicts CO profile well, as shown in Fig. 10(c).

We note that the Brequigny model and Mathieu model can't repeat the ignition delay time data well at low to intermediate temperature and the NO and CO concentration profiles at relatively lower temperature. While the Gao model shows good performance in predicting the ignition delay times and reasonable results in predicting the NO and CO concentration profiles. To further understand Gao model at low to intermediate temperature chemistry, chemical kinetic analysis has been conducted in the following.

3.4. Chemical kinetic analysis

3.4.1. Sensitivity analysis

Sensitivity analysis was conducted to identify the controlling reactions in predicting the auto-ignition process.

There are hundreds of reactions in the Gao model [27], as mentioned previously. The sensitivity coefficient of the ith reaction SC_i, is calculated through Eq. (4),

$$SC_i = (\tau_{2ki} - \tau_{0.5ki})/\tau_{ki} \quad (4)$$

where k_i is the rate constant of the ith reaction, τ_{ki} is the correspondingly computed ignition delay times. A negative SC_i indicates that increasing the rate constant k_i reduces the ignition delay time τ_{ki}, thus the ith reaction plays a promoting role for ignition, and vice versa. As such, by calculating and comparing the sensitivity coefficients for all the reactions, we can find out the most sensitive reactions for the ignition delay

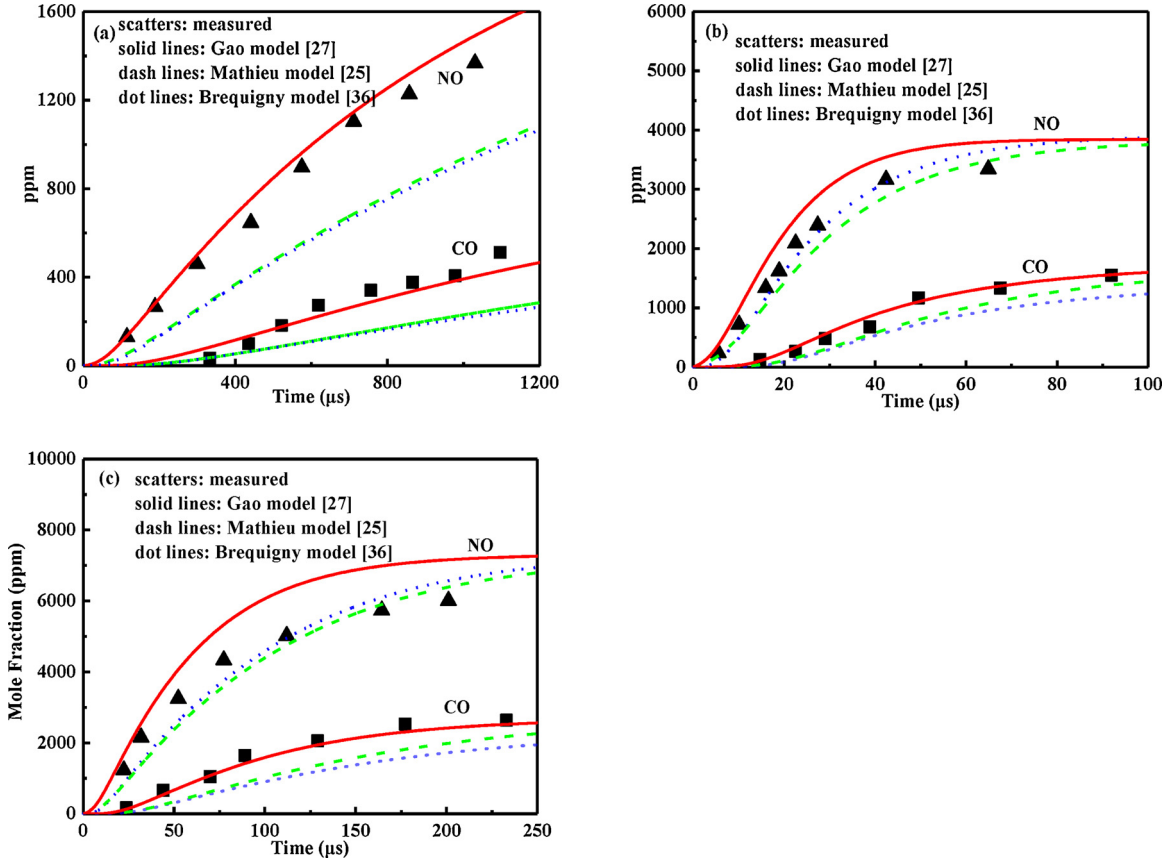

Fig. 10. Comparison of measured [21] and predicted concentrations of CO and NO in diluted shock tube decomposition of nitromethane. Experimental conditions: incident shock;(a): 0.25% CH_3NO_2/Ar mixture; T = 1051 K (NO) or 1057 K (CO); P = 0.83 atm; (b): 0.40% CH_3NO_2/Ar mixture; T = 1392 K (NO) or 1380 K (CO); P = 0.5 atm; (c): 0.76% CH_3NO_2/Ar mixture; T = 1243 K (NO) or 1236 K (CO); P = 0.69 atm (NO) or 0.65 atm (CO).

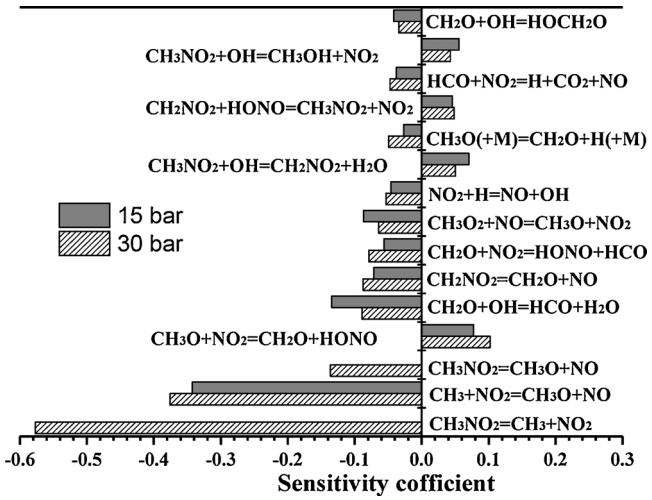

Fig. 11. Ignition delay time sensitivity for stoichiometric 2% NM mixture at T = 830 K, P_c = 15 bar and 30 bar by using the Gao model [27].

time simulation.

Fig. 11 shows the sensitivity analysis performed at 15 bar and 30 bar, 830 K, and 2.0% NM concentration for nitromethane by using the Gao model [27]. The top 15 sensitive reactions are presented in predicting the ignition delay times of nitromethane. It can be seen that the most sensitive reactions are $CH_3NO_2 = CH_3 + NO_2$, $CH_3 + NO_2 = CH_3O + NO$ and $CH_3NO_2 = CH_3O + NO$ at 30 bar, while only the reaction of $CH_3 + NO_2 = CH_3O + NO$ is the most sensitive at 15 bar. The decomposition reactions of nitromethane become insensitive as the pressure decreases. It will inhibit the ignition of nitromethane and increase the ignition delay times. Then the weak ignition, even non-ignition, will happen

3.4.2. Reaction pathway analysis

Reaction pathway during the nitromethane ignition process at the same condition with Fig. 11 is presented in Fig. 12. The diagram illustrates the main destruction channel of nitromethane at 20% NM consumption. It can be seen that the NM is primarily consumed by the unimolecular decomposition and H-abstraction reactions. The unimolecular decomposition, from the C–N bond breaking, results in 48% NM consumption. It is worth noting that importance of $CH_3NO_2 = CH_3 + NO_2$ is weakened at low temperature than that at high temperature [27]. The decomposition reaction of $CH_3NO_2 = CH_3O + NO$ consumes less than 1% nitromethane at this condition. Then H-abstraction reactions from methyl side consumes 39.2% nitromethane (most by OH radicals) to generate CH_2NO_2 and H_2. In the following, CH_3 radicals from the unimolecular decomposition are consumed via two main reaction pathways: the first (73.3%) in which CH_3 radicals are oxidized by NO_2 to form CH_3O radicals through $CH_3 + NO_2 = CH_3O + NO$, promoting reactivity; the second (25.0%) in which CH_3 radicals react with O_2 to form the peroxy radicals CH_3O_2, which readily react with NO to generate NO_2 and CH_3O radicals. Actually, the reaction of $CH_3O_2 + NO = CH_3O + NO_2$ makes an important role in promoting nitromethane oxidation [37]. The CH_3O radicals mainly go through: $CH_3O \rightarrow CH_2O \rightarrow CHO \rightarrow CO$ and, finally, will be oxidized to CO_2. For the other radical from the nitromethane decomposition, NO_2 is mainly consumed through $NO_2 + H{=}NO + OH$ (37.6%) and $NO_2 + CH_3 = CH_3O + NO$ (27.5%) to produce NO.

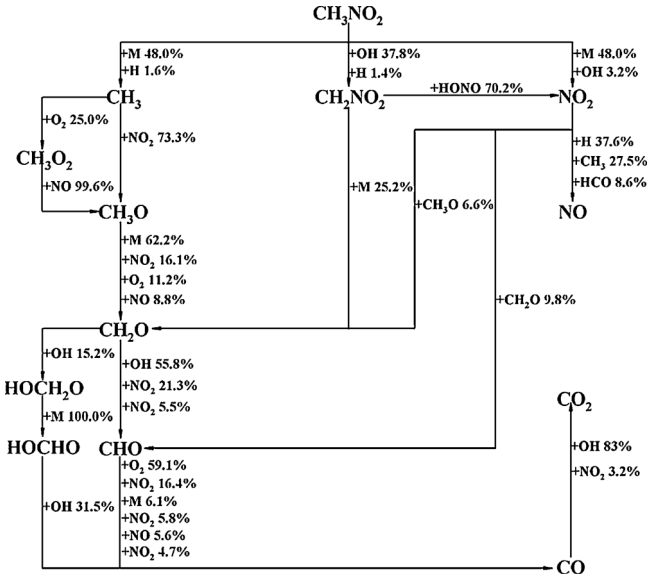

Fig. 12. Reaction pathway analysis for 830 K, [NM] = 2%, P_c = 30 bar, φ = 1.0, at 20% NM consumption using the Gao model [27].

3.5. Simulated critical conditions for nitromethane ignition

We further attempt to use the validated model to predict the critical conditions for nitromethane ignition at higher concentrations that are beyond the ability of the experimental facility. The adiabatic 0-dimensional homogeneous reactor is used, and Fig. 13 (a) and (b) shows the typical pressure evolution for the three types of ignition behavior and high NM concentration, respectively.

Fig. 14 presents the measured critical conditions at NM concentration of 1.0% and predicted ignition critical conditions at NM concentrations of 1.0%–30.0%. Firstly, compared the measurements and predictions at NM concentration of 1.0%, it can be found that the predicted critical temperature is lower than the measurements. This is reasonable because the simulation doesn't consider the heat loss, which will make the nitromethane mixture more difficult to be ignited at low temperature. However, the predicted results can qualitatively describe the critical condition for ignition and the trend with EOC pressure. Using this model, the safety performance of combustion, even explosion of nitromethane mixture at higher concentrations can be obtained. The critical conditions for NM concentrations of 5.0%–30.0% are simulated in the Fig. 14. It can be seen that the critical temperature for ignition decreases with the NM concentration increasing. In addition, at some NM concentration condition, the critical ignition temperature will decrease first and then keep constant with the EOC pressure increasing.

4. Concluding remarks

The auto-ignition behaviors of nitromethane in the low to intermediate temperature range 760–1025 K with different equivalence ratios (0.5–2.0), NM concentrations (0.5%–2.5%) and pressures (10–30 bar) have been investigated using a rapid compression machine. Firstly, the weakest thermodynamic conditions for the successful auto-ignition of the nitromethane containing mixture are determined. Results show that the rapid compression machine can provide fast compression with controlled pressure and temperature condition for evaluation of the thermo sensitivity of gaseous energetic material and present measurements for very dilute nitromethane mixture are also explosive under certain thermodynamic conditions. In addition, the ignition delay times for successful auto-ignition were measured. Results show that the dependence of nitromethane ignition on the equivalence ratio is weak. Subsequently, the measured ignition delay time data were compared with the numerical predictions by using several kinetic models in literature and our previous model [27] shows better agreement with measurements. Sensitivity analysis for the model reveals the importance of unimolecular decomposition and H-abstraction reactions for the ignition delay times in the temperature range studied herein. Finally, critical conditions for nitromethane ignition under extended

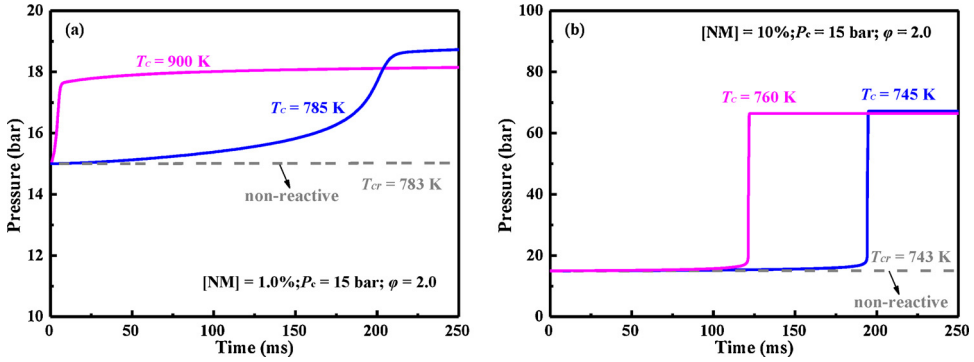

Fig. 13. Simulated typical pressure evolution: (a) the three types of ignition behavior at NM concentration of 1.0%; (b) ignition and non-ignition behavior at NM concentration of 10%.

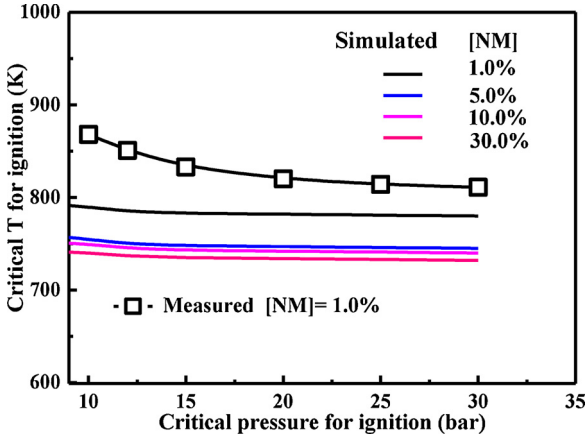

Fig. 14. Measured (scatters for 1.0% NM only) and predicted (lines) critical conditions for ignition for the equivalence ratio of 2.0.

conditions that are beyond the ability of the experimental facility were predicted.

Acknowledgements

This work is supported by the Science Challenge Project (No.TZ2016001), the National Natural Science Foundation of China (51722603), the Fundamental Research Funds for the Central Universities (Grant No.xjj2018174).

Appendix A. Supplementary data

Supplementary material related to this article can be found, in the online version, at doi:https://doi.org/10.1016/j.jhazmat.2019.05.036.

References

[1] P.C. Hsu, S.A. Strout, G.L. Klunder, E.M. Kahl, N.K. Muetterties, J.G. Reynolds, M. Gresshoff, Recent advances on thermal safety characterization of energetic materials, AIP Conf. Proc. 1979 (2018) 160010, https://doi.org/10.1063/1.5045009.

[2] L.U. Y.-C, A. Ulas, E. Boyer, K.K. Kuo, Determination of temperature profiles of self-deflagrating RDX by UV/Visible absorption spectroscopy and fine-wire thermocouples, Combust. Sci. Technol. 123 (1997) 147–163, https://doi.org/10.1080/00102209708935625.

[3] E. Boyer, K.K. Kuo, Modeling of nitromethane flame structure and burning behavior, Proc. Combust. Inst. 31 (2007) 2045–2053, https://doi.org/10.1016/j.proci.2006.07.025.

[4] T. Litzinger, M. Colket, M. Kahandawala, S.Y. Lee, D. Liscinsky, K. McNesby, R. Pawlik, M. Roquemore, R. Santoro, S. Sidhu, Fuel additive effects on soot across a suite of laboratory devices, Part 2: nitroalkanes, Combust. Sci. Technol. 183 (2011) 739–754, https://doi.org/10.1080/00102202.2010.539293.

[5] R.F. Cracknell, J.C.G. Andrae, L.J. Mcallister, M. Norton, H.L. Walmsley, The chemical origin of octane sensitivity in gasoline fuels containing nitroalkanes, Combust. Flame 156 (2009) 1046–1052, https://doi.org/10.1016/j.combustflame.2008.12.001.

[6] R. Guirguis, D. Hsu, D. Bogan, E. Oran, A mechanism for ignition of high-temperature gaseous nitromethane—the key role of the nitro group in chemical explosives, Combust. Flame 61 (1985) 51–62, https://doi.org/10.1016/0010-2180(85)90072-0.

[7] Q. Zhang, W. Li, D.C. Lin, N. He, Y. Duan, Influence of nitromethane concentration on ignition energy and explosion parameters in gaseous nitromethane/air mixtures, J. Hazard. Mater. 185 (2011) 756–762, https://doi.org/10.1016/j.jhazmat.2010.09.085.

[8] M.-O. Sturtzer, N. Lamoureux, C. Matignon, D. Desbordes, H.-N. Presles, On the origin of the double cellular structure of the detonation in gaseous nitromethane and its mixtures with oxygen, Shock. Waves 14 (2005) 45–51, https://doi.org/10.1007/s00193-004-0236-3.

[9] M. Bhowmick, E.J. Nissen, D.D. Dlott, Detonation on a tabletop: nitromethane with high time and space resolution, J. Appl. Phys. 124 (2018) 075901, , https://doi.org/10.1063/1.5043540.

[10] E.E. Fileti, V.V. Chaban, O.V. Prezhdo, Exploding nitromethane in silico, in real time, J. Phys. Chem. Lett. 5 (2014) 3415–3420, https://doi.org/10.1007/bf02515194.

[11] B. Lieberthal, W.R. Maines, D.S. Stewart, Predictions of detonation propagation through open cell foam embedded in chemically sensitized nitromethane, Propell. Explos. Pyrot. 42 (2017) 329–336, https://doi.org/10.1002/prep.201600060.

[12] T.R. Nelson, J.A. Bjorgaard, M.T. Greenfield, C.A. Bolme, K.E. Brown, S.D. Mcgrane, R.J. Scharff, S. Tretiak, Ultrafast photodissociation dynamics of nitromethane, J. Phys. Chem. A 120 (2016) 519–526, https://doi.org/10.1021/acs.jpca.5b09776.

[13] B. Leal-Crouzet, G. Baudin, H.N. Presles, Shock initiation of detonation in nitromethane, Combust. Flame 122 (2000) 463–473, https://doi.org/10.1016/S0010-2180(00)00132-2.

[14] R. Menikoff, M.S. Shaw, Modeling detonation waves in nitromethane, Combust. Flame 158 (2011) 2549–2558, https://doi.org/10.1016/j.combustflame.2011.05.009.

[15] B. Khasainov, H.N. Presles, D. Desbordes, Parametric study of double cellular detonation structure, Shock. Waves 23 (2013) 213–220, https://doi.org/10.1007/s00193-012-0419-2.

[16] E. Boyer, K. Kuo, Characteristics of nitromethane for propulsion applications, 44th AIAA Aerospace Sciences Meeting and Exhibit (2006) 361, https://doi.org/10.2514/6.2006-361.

[17] Q. Liu, C. Bai, L. Jiang, W.X. Dai, Deflagration-to-detonation transition in nitromethane mist/aluminum dust/air mixtures, Combust. Flame 157 (2010) 106–117, https://doi.org/10.1016/j.combustflame.2009.06.026.

[18] H.N. Presles, D. Desbordes, M. Guirard, C. Guerraud, Gaseous nitromethane and nitromethane-oxygen mixtures: a new detonation structure, Shock. Waves 6 (1996) 111–114, https://doi.org/10.1007/bf02515194.

[19] R.S. Zhu, M.C. Lin, CH3NO2 decomposition/isomerization mechanism and product branching ratios: an ab initio chemical kinetic study, Chem. Phys. Lett. 478 (2009) 11–16, https://doi.org/10.1016/j.cplett.2009.07.034.

[20] M. Isegawa, F. Liu, S. Maeda, K. Morokuma, Ab initio reaction pathways for photo dissociation and isomerization of nitromethane on four singlet potential energy surfaces with three roaming paths, J. Chem. Phys. 140 (2014) 244310, https://doi.org/10.1063/1.4883916.

[21] D.S.Y. Hsu, M.C. Lin, Laser probing and kinetic modeling of NO and CO production in shock-wave decomposition of nitromethane under highly diluted conditions, J. Energ. Mater. 3 (1985) 95–127, https://doi.org/10.1080/07370658508012337.

[22] P. Glarborg, A.B. Bendtsen, J.A. Miller, Nitromethane dissociation: Implications for the CH3 + NO2 reaction, Int. J. Chem. Kinet. 31 (1999) 591–602, https://doi.org/10.1002/(SICI)1097-4601(1999)31:9<591::AID-KIN1>3.0.CO;2-E.

[23] C.J. Annesley, J.B. Randazzo, S.J. Klippenstein, L.B. Harding, A.W. Jasper, Y. Georgievskii, B. Ruscic, R.S. Tranter, Thermal dissociation and roaming isomerization of nitromethane: experiment and theory, J. Phys. Chem. A 119 (2015) 7872–7893, https://doi.org/10.1021/acs.jpca.5b01563.

[24] A. Matsugi, H. Shiina, Thermal decomposition of nitromethane and reaction between CH3 and NO2, J. Phys. Chem. A 121 (2017) 4218, https://doi.org/10.1021/acs.jpca.7b03715.

[25] O. Mathieu, B. Giri, A.R. Agard, T.N. Adams, J.D. Mertens, E.L. Petersen, Nitromethane ignition behind reflected shock waves: experimental and numerical study, Fuel 182 (2016) 597–612, https://doi.org/10.1016/j.fuel.2016.05.060.
[26] J.D. Nauclér, Y. Li, E.J.K. Nilsson, H.J. Curran, A.A. Konnov, An experimental and modeling study of nitromethane + O2 + N2 ignition in a shock tube, Fuel 186 (2016) 629–638, https://doi.org/10.1016/j.fuel.2016.09.003.
[27] Z.Q. Gao, M. Yang, C.L. Tang, F.Y. Yang, K. Yang, R. Yang, Z.H. Huang, Measurements of the high temperature ignition delay times and kinetic modeling study on oxidation of nitromethane, Combust. Sci. Technol. (2019), https://doi.org/10.1080/00102202.2019.1565533.
[28] Y. Liu, C.L. Tang, Y.T. Wu, M. Yang, Z.H. Huang, Low temperature ignition delay times measurements of 1,3,5-trimethylbenzene by rapid compression machine, Fuel 241 (2019) 637–645, https://doi.org/10.1016/j.fuel.2018.12.077.
[29] J.P. Mccullough, D.W. Scott, R.E. Pennington, I.A. Hossenlopp, G. Waddington, Nitromethane: the vapor heat capacity, heat of vaporization, vapor pressure and gas imperfection; the chemical thermodynamic properties from 0 to 1500°K, J. Am. Chem. Soc. 76 (1954) 175–186, https://doi.org/10.1021/ja01648a008.
[30] D. Darcy, H. Nakamura, C.J. Tobin, M. Mehl, W.K. Metcalfe, W.J. Pitz, C.K. Westbrook, H.J. Curran, A high-pressure rapid compression machine study of n -propylbenzene ignition, Combust. Flame 161 (2014) 65–74, https://doi.org/10.1016/j.combustflame.2013.08.001.
[31] B.W. Weber, C.J. Sung, Comparative autoignition trends in butanol isomers at elevated pressure, Energy Fuel. 27 (2013) 1688–1698, https://doi.org/10.1021/ef302195c.
[32] H. Di, X. He, P. Zhang, Z. Wang, M.S. Wooldridge, C.K. Law, C. Wang, S. Shuai, J. Wang, Effects of buffer gas composition on low temperature ignition of iso-octane and n-heptane, Combust. Flame 161 (2014) 2531–2538, https://doi.org/10.1016/j.combustflame.2014.04.014.
[33] N. Xu, Y. Wu, C. Tang, P. Zhang, X. He, Z. Wang, Z. Huang, Experimental study of 2,5-dimethylfuran and 2-methylfuran in a rapid compression machine: comparison of the ignition delay times and reactivity at low to intermediate temperature, Combust. Flame 168 (2016) 216–227, https://doi.org/10.1016/j.combustflame.2016.03.016.
[34] B.W. Weber, C.J. Sung, M.W. Renfro, On the uncertainty of temperature estimation in a rapid compression machine, Combust. Flame 162 (2015) 2518–2528, https://doi.org/10.1016/j.combustflame.2015.03.001.
[35] S.B. Markofsky, Nitro Compounds Aliphatic, Wiley-VCH, Germany, 2011.
[36] P. Brequigny, G. Dayma, F. Halter, C. Mounaïm-Rousselle, T. Dubois, P. Dagaut, Laminar burning velocities of premixed nitromethane/air flames: an experimental and kinetic modeling study, Proc. Combust. Inst. 35 (2015) 703–710, https://doi.org/10.1016/j.proci.2014.06.126.
[37] J.C. Tricot, A. Perche, M. Lucquin, Gas phase oxidation of nitromethane, Combust. Flame 40 (1981) 269–291, https://doi.org/10.1016/0010-2180(81)90130-9.